

Impact of the C-Terminal Loop of Histidine Triad Nucleotide Binding Protein1 (Hint1) on Substrate Specificity

Tsui-Fen Chou,[‡] Yuk Y. Sham,[§] and Carston R. Wagner^{*,‡,§,||}

Departments of Medicinal Chemistry and Chemistry, Supercomputer Institute, University of Minnesota, Minneapolis, Minnesota 55455

Received June 24, 2007; Revised Manuscript Received September 1, 2007

ABSTRACT: Although highly sequence similar, human histidine triad nucleotide binding protein (hHint1) and *E. coli* hinT (*echinT*) exhibit significant differences in their phosphoramidase substrate specificity and lysyl-adenylate hydrolytic activity. Observing that the C termini of each enzyme are highly dissimilar, we created two chimeric Hint's: one in which the C terminus of hHint1 was replaced with the C terminus of *echinT* (*Hs/ec*) and the other in which the C terminus of *echinT* was replaced with the C terminus of hHint1 (*ec/Hs*). The *Hs/ec* chimera exhibited nearly identical specificity constants (k_{cat}/K_m) to those found for *echinT*, whereas the specificity constants of the *ec/Hs* chimera were found to approximate those for hHint1. In particular, as observed for *echinT*, the *Hs/ec* chimera does not exhibit a preference for phosphoramidates containing D- or L- tryptophan, while the *ec/Hs* chimera adopts the human enzyme preference for the L configuration. In addition, the studies with each chimera revealed that differences in the ability of hHint1 and *echinT* to hydrolyze lysyl-AMP generated by either *E. coli* or human lysyl-tRNA synthetase were partially transferable by C-terminal loop exchange. Hence, our results support the critical role of the C-terminal loop of human and *E. coli* Hint1 on governing substrate specificity.

Histidine triad nucleotide binding protein (Hint¹) is a ubiquitous purine nucleoside phosphoramidase which catalyzes the hydrolysis of the phosphoramidate bond between a nucleoside monophosphate and an amine leaving group (1, 2). The phosphoramidase activity of Hints has been proposed as the bioactivating enzyme for antiviral and anticancer phosphoramidate pronucleotides (2, 3). Recently, aminoacyl-AMP and acyl-AMP have been shown to be the first potential natural substrates for Hints (4, 5). Hint is conserved from bacteria to human and considered to be the ancestor of the histidine triad protein superfamily (HIT), which contains the highly conserved motif His-X-His-X-His-XX, where X is a hydrophobic residue (6). It has been recently demonstrated by an affinity tag purification followed by mass spectroscopy proteomic analysis that *echinT* forms stable potential protein:protein interactions with six species: a putative oxidoreductase and formate dehydrogenase (b1501), the heat shock protein 70 (Hsp70), the β -subunit of DNA polymerase III (dnaN), a membrane-bound lytic murein transglycosylase D (dniR), ET-Tu elongation factor (tufA), and a putative synthetase (yjhH) (7). In addition, *Mycoplasma* HinT has been shown to interact with two membrane proteins (P60 and P80) (8, 9). However, the physiological and biochemical importance of these interactions has remained unresolved. Recently, we demonstrated

that *echinT* appears to be important for cell growth under high salt conditions (2).

E. coli contains only one hinT gene, whereas three Hint genes (hHint1, hHint2, hHint3) have been identified in human tissue (2, 6). Accumulated evidence has pointed to the potential function of eukaryotic Hint1 on the regulation of transcriptional processes through interactions with important transcriptional factors. For instance, hHint1 has been isolated in a complex with lysyl-tRNA synthetase and the transcription factors, microphthalmia or USF2 (10, 11). In addition, hHint1 was identified as a direct interaction partner with human Pontin and Reptin in the TCF- β -catenin transcription complex (12). Moreover, Hint1 was previously reported to interact with cyclin-dependent kinase 7 (CDK7), providing further evidence of its potential function in growth control and transcriptional regulation (13). Both hHint1 and hHint2 have been implicated in the regulation of apoptosis, which provided one mechanism for their tumor suppressor activities (14, 15).

To gain insights into the origin of the differential kinetic behavior between the human and *E. coli* enzymes, the amino acid sequences of both enzymes were compared. Although *echinT* and hHint1 share nearly 50% sequence similarity, the C-termini are not sequence similar nor of the same length. (Figure 1). On the basis of the X-ray crystal structures of human and rabbit Hint1, a homology model of *echinT* was generated, revealing that as observed for the mammalian enzymes the C-terminus of *echinT* is likely to lie in close proximity to the active site (16–18). Consequently, we hypothesized that our recent observation of substrate specificity differences between the bacterial and human Hints for nucleoside phosphoramidates and lysyl-AMP may in part

* To whom correspondence should be addressed. Phone: 612-625-2614. Fax: 612-624-0139. E-mail: wagne003@umn.edu.

[‡] Department of Medicinal Chemistry.

[§] Supercomputer Institute.

^{||} Department of Chemistry.

¹ Abbreviations: *echinT*, *E. coli* hinT; ecLysU, *E. coli* LysRS; Hint1, histidine triad nucleotide binding protein1; hHint1, human Hint1; HIT, histidine triad; LysRS, lysyl-tRNA synthetase; HsLysRS, human LysRS.

hHint: MADEIAKAQVARPGGDTIFGKIIRKEIPAKIIFEDDRCLAFHDISPQAPT
 echinT: MAEE-----TIFSKIIRREIPSDIVYQDDLVTAFRDISPQAPT

hHint: HFLVIPKKHISQISVAEDDESLLGHLMIIVGKKCAADLGLNK-GYRMVVN
 echinT: HILIIIPNIIPTVNDVSAEHEQALGRMITVAAKIAEQEGIAEDGYRLIMN

hHint: EGSDDGGQSVYHVLHVLGGRRQHWPPG
 echinT: TNRHGGQEVYHIHMHLLGGRLGPMLAHKGL

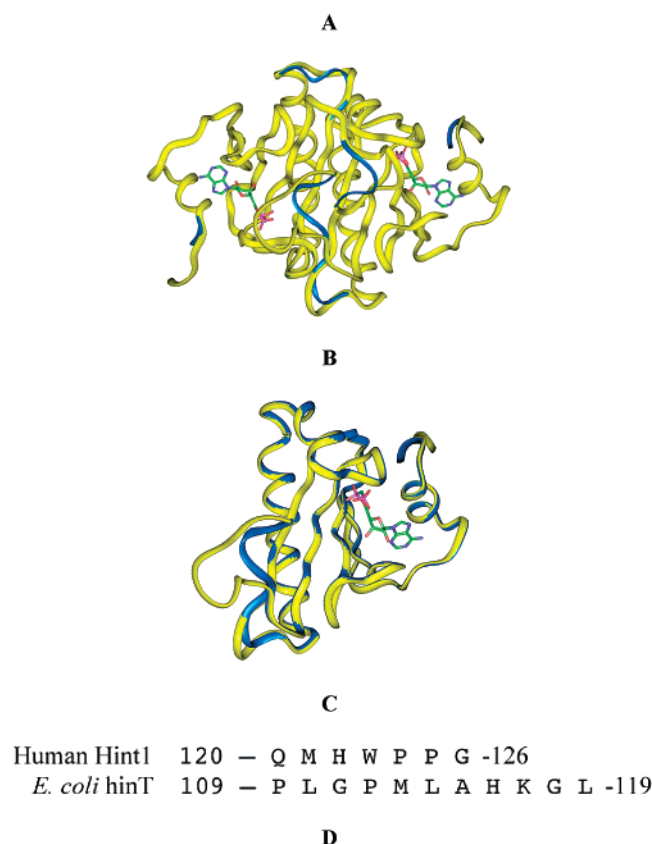


FIGURE 1: Homology Model of *echinT*. (A) Sequence alignment between human Hint1 and *echinT* indicated that the two proteins share high homology; the conserved region is highlighted in bold, (B) superimposition of dimeric hHint1 crystal structure (blue, PDB code: 1AV5) (17) and homology model of *echinT* (yellow), (C) superimposition of one monomer of hHint1 and *echinT* model, (D) the exchanged C-terminal regions of hHint1 and *echinT*.

result from differences in the C termini. To address this possibility, two chimeric Hints were created: one in which the C terminus of hHint1 (Gln120 to Gly126) was replaced with the C terminus of *echinT* (Pro109 to Leu119) (Hs/*ec*) and one in which the C terminus of *echinT* was replaced with the C terminus of hHint1 (*ec*/Hs). The Hs/*ec* chimera and *echinT* displayed almost identical substrate specificities against 12 phosphoramidate substrates, while the *ec*/Hs chimera exhibited specificity constants similar to those found for hHint1. Furthermore, as observed for *echinT*, the amount of adenylated enzyme intermediate formed after hydrolysis by Hs/*ec* chimera of lysyl-AMP generated by *E. coli* LysU and HsLysRS was shown to be enhanced relative to hHint1. In contrast, the amount of intermediate formed by the *ec*/Hs chimera and *echinT* were similar for HsLysRs but not *ec*LysU (4). Taken together, these results provide the first evidence that alterations in the C-terminal domain contribute to the differential substrate specificity observed between *E. coli* and human Hints.

MATERIALS AND METHODS

Homology Modeling. All modeling was performed using the homology modeling module of the INSIGHTII software package (Accelrys, Inc.). Comparisons among various known structures of human and rabbit Hint1 proteins suggested very high sequence similarity and structure conservation within the Hint1 family of proteins (16–18). Thus, homology modeling was carried out to model the structure of *echinT* protein. The crystal structure of the hHint1 protein dimer (17) was obtained from the Protein Data Bank (PDB code: 1AV5) and used as the structural template for the homology modeling. The structurally conserved regions (SCR) of hHint1, rHint1, and *echinT* were first identified by multiple sequence alignment. The Cartesian coordinates for the aligned SCR for *echinT* were assigned using the hHint1 structure as the template. All nonstructurally conserved regions (nSCR) were assigned using the loop generation feature of the homology modeling module. The loop generation of the C-terminus of *echinT* was restricted to include a C-terminus to C-terminus interaction as observed in the hHint1 protein dimer. The final structure was energy minimized by the molecular mechanics method using the steepest descent algorithm for 1000 steps.

Plasmid Construction by Domain-Swap Mutagenesis. The hHint1/*E. coli* chimera mutant (Hs/*ec* chimera) was generated with the wild-type vector “hHint1-pSGA02” using a Quick-Change mutagenesis kit (Stratagene) with primers 5'-CT-TGGAGGTCTCGCCCGCTGGGACCAATGCTG-GCGCATAAAGGTCTGTAACCTCGAGGGTACCCATGG-3' and 5'-CCATGGGTACCCTCGAGTTACAGACCTTTATGCGCCAGCATTGGTCCCAGCGGCCGACCTCCAAG-3'. The reciprocal chimera (*ec*/Hs chimera) was generated with the wild-type vector “*echinT*-pSGA02” (2) with primers 5'-GCACTTGTTGGGTGGCCGTCAAATGCAT-TGGCCTCCTGGTTAACTCGAGGGTAC-3' and 5'-GTAC-CCTCTGAGTTAAACAGGAGGCCAATG-CATTTGACGGCCACCAACAAGTGC-3'.

Expression and Purification of Recombinant Proteins. To avoid possible wild-type *E. coli* hinT contaminant, plasmids were transformed into *E. coli* hinT disrupted strain BB2 as described (2). Cell growth and cell lysates extractions were described previously (2). Human Hint1, *echinT*, or the chimeras were purified by an AMP-agarose affinity column (Sigma) followed by a PD-10 desalting column as previously described (1). The purified enzyme was exchanged to buffer A (20 mM Tris pH 7.0, 1 mM EDTA, 1 mM DTT) and concentrated with an Amicon stirred cell with a YM-3 membrane (Millipore). Homogeneity was analyzed by SDS-PAGE and gel filtration chromatography (2). Protein concentrations were determined with the Bradford protein assay (Biorad). The apparent molecular weight of recombinant purified proteins was analyzed by analytical gel filtration chromatography on the Superdex G75 column (GE Biosciences), and the proteins eluted with P500 buffer (0.5 M NaCl, 50 mM potassium phosphate, 1 mM EDTA, pH 7.0) as previously described (2).

Circular Dichroism (CD) Spectroscopy. CD spectra of proteins were obtained at 23 °C with a J710 spectropolarimeter (Jasco). Proteins at concentrations of 10 μ M in sodium phosphate buffer (10 mM, pH 7.2) were analyzed in a quartz cuvette with a path length of 1 mm, and spectra

were accumulated and averaged over nine scans. Subtraction of buffer background from the protein spectrum was performed using Excel (Microsoft).

Steady-State Kinetics of the Chimera with the Fluorescent Phosphoramidase Assay. Hydrolysis of the fluorogenic substrates by the chimera mutant was carried out in degassed HEPES buffer (20 mM HEPES, pH 7.2, 1 mM MgCl₂, 600 μ L) in quartz cuvettes as previously described (19). Initial velocities were determined with six different concentrations of each substrate. All the kinetic assays were performed in duplicate at 25 °C with optimal amounts of the enzymes ranging from 0.5 to 1000 pmol. The reactions were monitored over a linear period of time. The Michaelis–Menten constants, k_{cat} (s⁻¹) and K_m (μ M), were determined by nonlinear regression analysis of the initial velocity versus concentration using JUMP IN. Substrate specificity was expressed by the second-order rate constant k_{cat}/K_m (s⁻¹ M⁻¹ $\times 10^{-3}$) and variance expressed as standard deviations.

Adenylation of Hints by *E. coli* and Human LysRSs. The adenylation reaction was carried as described (4, 5). *E. coli* LysRS (*ecLysU*, 0.1 μ M) or HsLysRS (0.9 μ M) was incubated with [α -³²P]-ATP (0.9 μ M, 800 Ci/mmol, MP Biomedicals) in buffer A (7 μ L, 25 mM Tris HCl, pH 7.8, 100 mM NaCl, 2 mM MgCl₂, 1 mM DTT, 28.5 μ M lysine) with or without yeast inorganic pyrophosphatase (0.02 U/ μ L) at 23 °C for 1 min followed by addition of proteins (final concentration is 3.6 μ M) and incubated for an additional 1 min. The reaction was terminated by addition of SDS sample buffer (4 \times , 4 μ L, Invitrogen). The reaction mixture was heated for 10 min at 80 °C, and the proteins were separated by SDS-PAGE and electroblotted onto a polyvinylidene difluoride (PVDF) membrane. Labeled proteins were visualized by subjecting dried PVDF membranes to autoradiography with a storage phosphor screen for 14 h followed by scanning with a Storm 840 Phosphorimager. Quantitation of the intensity of the ³²P signal was carried out with ImageQuant software (GE Healthcare).

RESULTS

Homology Modeling. The sequence alignment between hHint1 and *echinT* is shown in Figure 1A, and the SCR is highlighted in bold. The nonconserved C terminus of *echinT* was generated with the loop generation feature under the homology modeling module, and the flexibility of this loop was then constrained based upon the salt bridge between Gly126 of one monomer and Arg119 of the other monomer, enabling us to obtain the initial structure after energy minimization. The final minimized structure was superimposed with hHint1 as shown in Figure 1B. Only one superimposed monomer is shown in Figure 1C, clearly demonstrating the larger C terminus of the *echinT* model.

Plasmid Construction and Protein Purification of the Chimeras. To evaluate the proposed role of the C terminus, a plasmid for overexpressing the recombinant Hs/*ec* chimera mutant was generated by PCR-based mutagenesis with wild-type hHint1-pSGA02 plasmid (20) and two 66 bp primers containing 33 bp corresponding to the C terminus of *echinT* (a.a. 109–119) and 33 bp complementary to the hHint1-pSGA02 plasmid. The chimera was isolated after expression in an *echinT* minus strain and the protein purity verified by SDS-PAGE (Supporting Information, Figure 1A, lane 1) and

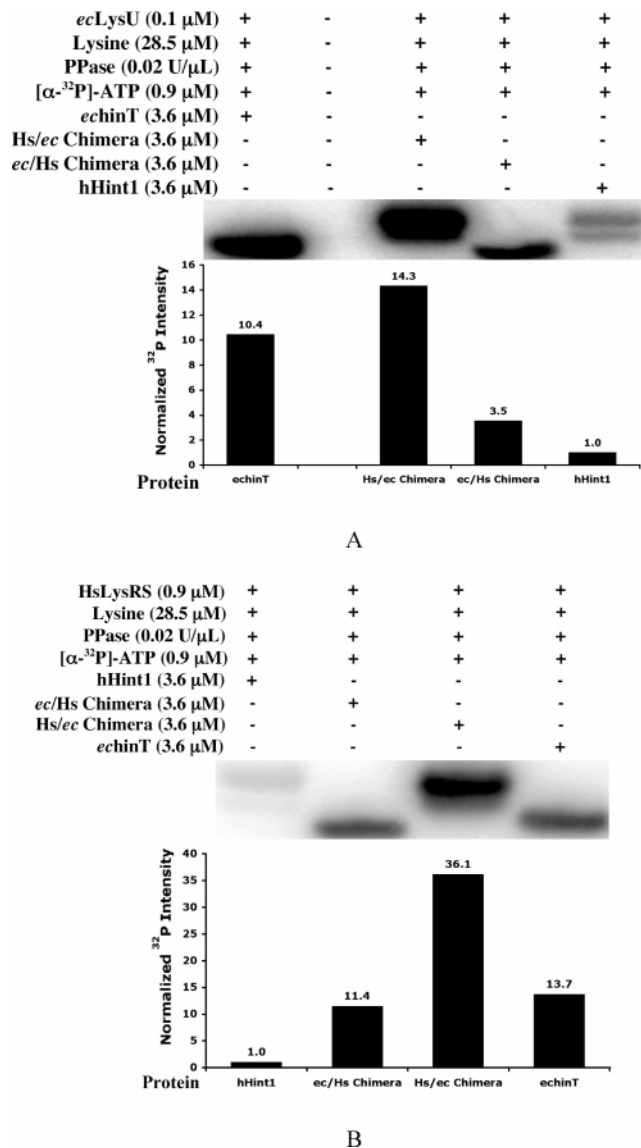
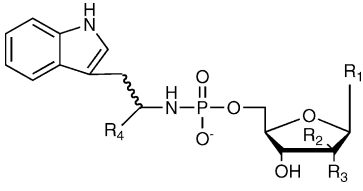


FIGURE 2: Adenylation of Hints by *ecLysU* and HsLysRS. Labeling was carried out in buffer A containing lysine (28.5 μ M), and PPase (0.02 unit/ μ L) with [α -³²P]-ATP (0.9 μ M) at 23 °C for 1 min followed by addition of Hint proteins (3.6 μ M) for 1 min with, (A) *ecLysU* (0.1 μ M) and (B) HsLysRS (0.9 μ M).

gel filtration analysis with a Superdex 75 10/300GL column (GE Healthcare). The retention time at 22.7 min of the elution chromatography (Supporting Information, Figure 1B) indicated formation of the homodimer of the Hs/*ec* chimera in solution based on the molecular weight calibration curve (Supporting Information, Figure 2) prepared as previously described (2). The reciprocal *ec*/Hs chimera was generated with the wild-type *echinT*-pSGA02 plasmid and primers encoding the amino acid sequence corresponding to the human C terminus (a.a.120–126). The recombinant purified *ec*/Hs chimera was shown to be homogeneous by SDS-PAGE (Supporting Information, Figure 1A, lane 4).

Secondary Structure Analysis. CD spectra of the Hint proteins were determined in the far-UV region (190–260 nm). The result was expressed as the mean residue ellipticity (MRE). As can be seen in the CD spectra for hHint1 (black square), *echinT* (yellow diamond), and the Hs/*ec* chimera (blue triangle) are superimposable and consistent with a nearly identical combination of α -helical and β -sheet

Table 1: Steady-State Kinetic Parameters of hHint1, *echinT*, and the Hs/*ec* Chimera and *ec*/Hs Chimera^a


Compound Number	R ₁	R ₂	R ₃	R ₄	k_{cat} (s ⁻¹)			
					hHint1 ^b	<i>echinT</i> ^b	Hs/ <i>ec</i> Chimera	<i>ec</i> /Hs Chimera
1	Adenine	H	OH	<i>S</i> -COOCH ₃	0.012 ± 0.001	1.1 ± 0.1	0.012 ± 0.002	0.49 ± 0.06
2	Adenine	H	OH	<i>R</i> -COOCH ₃	0.27 ± 0.02	1.0 ± 0.2	0.022 ± 0.004	1.8 ± 0.3
3	Adenine	H	OH	H	2.1 ± 0.1	4.5 ± 0.07	0.10 ± 0.002	12 ± 1
4	Adenine	OH	H	H	1.1 ± 0.03	1.5 ± 0.4	0.26 ± 0.02	ND
5	Guanine	H	OH	<i>S</i> -COOCH ₃	0.007 ± 0.002	0.5 ± 0.02	0.026 ± 0.001	0.13 ± 0.03
6	Guanine	H	OH	<i>R</i> -COOCH ₃	0.26 ± 0.02	0.37 ± 0.01	0.022 ± 0.0003	ND
7	Guanine	H	OH	H	2.3 ± 0.07	4.0 ± 0.4	0.10 ± 0.03	12 ± 2
8	7-Benzyl-Guanine	H	OH	H	0.68 ± 0.04	0.15 ± 0.01	0.039 ± 0.003	ND
9	Hypoxanthine	H	OH	H	2.6 ± 0.04	4.2 ± 0.1	0.10 ± 0.003	ND
10	Uracil	H	OH	H	2.5 ± 0.3	2.4 ± 0.6	0.093 ± 0.003	ND
11	Cytosine	H	OH	H	1.2 ± 0.1	0.49 ± 0.03	0.058 ± 0.002	ND
12	Thymine	H	H	H	0.10 ± 0.01	0.02 ± 0.002	0.014 ± 0.002	ND

Compound Number	R ₁	R ₂	R ₃	R ₄	K_{m} (μM)			
					hHint1 ^b	<i>echinT</i> ^b	Hs/ <i>ec</i> Chimera	<i>ec</i> /Hs Chimera
1	Adenine	H	OH	<i>S</i> -COOCH ₃	41 ± 4	43 ± 3	0.32 ± 0.03	100 ± 14
2	Adenine	H	OH	<i>R</i> -COOCH ₃	4.1 ± 0.9	45 ± 12	0.67 ± 0.09	18 ± 4
3	Adenine	H	OH	H	0.13 ± 0.02	5.2 ± 0.2	0.12 ± 0.01	1.3 ± 0.2
4	Adenine	OH	H	H	1.0 ± 0.06	60 ± 19	2.9 ± 0.4	ND
5	Guanine	H	OH	<i>S</i> -COOCH ₃	31 ± 1	32 ± 3	0.7 ± 0.2	80 ± 25
6	Guanine	H	OH	<i>R</i> -COOCH ₃	3.3 ± 0.6	21 ± 1	0.83 ± 0.05	ND
7	Guanine	H	OH	H	0.21 ± 0.02	6 ± 1	0.17 ± 0.01	2.8 ± 0.7
8	7-Benzyl-Guanine	H	OH	H	14 ± 2	56 ± 6	17 ± 3	ND
9	Hypoxanthine	H	OH	H	0.71 ± 0.03	14 ± 1	0.53 ± 0.04	ND
10	Uracil	H	OH	H	2.2 ± 0.4	42 ± 15	0.87 ± 0.07	ND
11	Cytosine	H	OH	H	2.3 ± 0.4	30 ± 3	1.53 ± 0.09	ND
12	Thymine	H	H	H	32 ± 5	46 ± 7	53 ± 12	ND

^a Measurements were carried out in duplicate and variants are given as standard deviations. ^b Data for hHint1 and *echinT* was adapted from ref 19.

Table 2: Comparison of the Second-order Rate Constants ($k_{\text{cat}}/K_{\text{m}}$) for hHint1, *echinT*, and the Hs/*ec* Chimera and the *ec*/Hs Chimera.

Compound Number	$k_{\text{cat}}/K_{\text{m}}$ (s ⁻¹ /M ⁻¹ × 10 ⁻³)			
	hHint1 ^a	<i>echinT</i> ^a	Hs/ <i>ec</i> Chimera	<i>ec</i> /Hs Chimera
1	0.23 ± 0.04	28 ± 4	38 ± 4	5 ± 2
2	70 ± 20	20 ± 10	33 ± 6	100 ± 60
3	15000 ± 3000	870 ± 50	830 ± 50	9100 ± 2600
4	1100 ± 100	30 ± 20	90 ± 20	ND
5	0.23 ± 0.01	16 ± 2	40 ± 10	2 ± 1
6	80 ± 30	17 ± 2	27 ± 2	ND
7	11000 ± 1000	700 ± 200	580 ± 50	4600 ± 2500
8	50 ± 10	2.6 ± 0.7	2.3 ± 0.6	ND
9	3700 ± 300	310 ± 40	190 ± 20	ND
10	1200 ± 500	70 ± 60	110 ± 10	ND
11	600 ± 200	20 ± 4	40 ± 4	ND
12	3 ± 1	0.4 ± 0.2	0.3 ± 0.1	ND

^a Data for hHint1 and *echinT* was adapted from ref 19.

secondary structural elements (Supporting Information, Figure 3).

Chimera Mutants Switched Substrate Specificity. The fluorogenic indole-containing substrates examined in this study were synthesized as previously reported (Table 1) (19). This continuous assay enables the Michaelis–Menten parameters for Hint proteins to be easily determined (19). Moreover, tryptophan nucleoside phosphoramidates, which

incorporate the fluorescent indole moiety, have been shown to have potent antiviral and anticancer activity (21). The steady-state kinetic results of the chimera mutants are summarized in Tables 1 and 2 and compared to the previously reported results for hHint1 and *echinT*. In spite of 47% amino acid sequence identity between hHint1 and *echinT*, differences in substrate specificity are clearly evident. Briefly, *echinT* displayed K_{m} values 1–2 orders of magnitude

greater than those for hHint1 except for compounds 1, 5, 8, and 12, while the second-order rate constant (k_{cat}/K_m) for hHint1 was found to be 10-fold greater than that of *echinT*. The key difference between the enzymes is that hHint1 clearly exhibits a preference by a factor of 300 for substrates containing amino acids with a D configuration, whereas the *E. coli* enzyme processes D- and L-amino acid containing substrates similarly (19). The Hs/*ec* chimera and *E. coli* enzymes display highly similar substrate specificities based on the k_{cat}/K_m values, particularly with regard to the D substrates, whereas the *ec*/Hs chimera and hHint1 not only exhibit similar k_{cat}/K_m values but also a preference for D substrate (compound 2) over L substrate (compound 1) (Table 2, Supporting Information Figure 4). Nevertheless, in general a decrease by an order of magnitude in the k_{cat} values and similar increase in the K_m values for the Hs/*ec* chimera when compared to hHint1 was observed (Table 1). In contrast, the k_{cat} values for the *ec*/Hs chimera were found not to be adversely affected by the hHint1 C terminus. In two cases, compounds 1 and 5, the human C terminus resulted in a moderate reduction in k_{cat} . Interestingly, while for compounds 3 and 7 the expected decrease in the K_m values was observed, the k_{cat} values were increased by approximately 4-fold. In addition, a similar trend for hHint1 and the *ec*/Hs chimera was observed for the k_{cat} and K_m values when compounds 1–3 and 5 and 7 were used as substrates.

Adenylation of Hints by Human and *E. coli* LysRS. Recently, we have shown that lysyl-AMP generated by LysRS is a native substrate for hHint1 and *echinT*. During the reaction the active site nucleophile, His112 of hHint1, is adenylated in situ (Supporting Information, Figure 5) (4). Additionally, adenylation of the Hs/*ec* chimera has been shown to be similar to that for *echinT* (4). Therefore, the ability of the *ec*/Hs chimera to utilize lysyl-AMP as a substrate was examined (Figure 2). As shown in Figure 2A, the intensity of the labeling of the *ec*/Hs chimera by *ec*LysU was found to decrease by 3-fold when compared to *echinT* labeling. Similar to the studies carried out with *ec*LysU, adenylation of Hs/*ec* by HsLysRS was enhanced when compared to hHint1 (Figure 2B). In contrast, the hHint1 C terminus had little effect on the adenylation of *ec*/Hs when compared to *echinT*. Consistent with the phosphoramidate steady-state kinetic results of both engineered chimeric mutants (Table 2, Supporting Information Figure 4) the C terminus of both hHint1 and *echinT* exhibited a controlling influence on their aminoacyl-AMP hydrolase substrate specificity.

DISCUSSION

In spite of the fact that bovine Hint1 has been known since 1990 (22), Hint is the only subfamily of HIT with an ill-defined cellular function. Studies of knock-out mice have provided evidence that Hint1 may function as a tumor suppressor (23–25), but the mechanism by which Hint1 suppresses tumor formation is not clear. Protein–protein interaction studies of mammalian Hint1 suggest that its role in regulating transcription by directly binding either to the basic transcriptional machinery (13) or to specific complexes of transcription factors in the nucleus (10, 11). Although, the relevance of the catalytic activity of Hint1 to these biological processes remains ambiguous, the potential utility of Hints for the bioactivation of antiviral, antibacterial, and

anticancer phosphoramidate pronucleotides is of considerable interest (2, 3, 19). In addition to their phosphoramidase activity, we recently demonstrated that both hHint1 and *echinT* efficiently hydrolyze the lysyl-AMP intermediate formed by both the bacterial and human lysyl-tRNA synthetases prior to tRNA charging (4). Studies with the Hs/*ec* chimera clearly demonstrated that the C termini of the bacterial and human Hints have differential effects on lysyl-AMP hydrolysis. Consequently, we chose to contrast and compare the effect of the C termini of each enzyme on the phosphoramidase substrate specificity and lysyl-AMP hydrolyase with human/*E. coli* (Hs/*ec*) and *E. coli*/human (*ec*/Hs) chimeric proteins.

In our recent structure–activity relationship study of hHint1 and *echinT* with a series of phosphoramidate and phosphoramidothioates substrates we demonstrated that *echinT* can tolerate a wider range of substrates than hHint1 (19). If sterically hindered substrates (compounds 1, 2, 5, 6) are not considered, hHint1 is a more efficient catalyst by factors of 3–32-fold (Table 2). The engineered Hs/*ec* chimera, which contains 92% of the human amino acid sequence and 8% of the *echinT* sequence, was constructed by deleting the C terminus of hHint1 and simultaneously inserting the C terminus of *echinT* (Figure 1D). As shown in Figure 2, the Hs/*ec* chimera exhibited nearly identical k_{cat}/K_m values to those observed for *echinT*. Similarly the *ec*/Hs chimera, which contains 94% of the *echinT* amino acid sequence and 6% of the hHint1 sequence, exhibited k_{cat}/K_m values approximately the same as those observed for hHint1. Nevertheless, the bacterial C terminus tended to decrease hHint1 turnover and K_m values, while the human C terminus increased the turnover number of *echinT* but generally decreased K_m . The differential effects of the C-terminal domains suggests that this region of the protein has a broad ability to influence Hint catalysis in a species-specific manner. Consistent with these findings, the enhanced adenylation of *echinT* by lysyl-tRNA synthetases relative to hHint1 is also observed for the Hs/*ec* chimera, while a decrease in adenylation was observed for the *ec*/Hs chimera (Figure 2) (4). In addition, the results of molecular modeling studies, placing the C terminus of *echinT* near the enzyme's active site, are supportive of a role for this domain in influencing Hint catalysis.

In summary, we reported the first biochemical evidence for the significance of the C terminus of Hint1 proteins in mediating their phosphoramidate and acyl-AMP hydrolyase activity. The C-terminal motif of Hint proteins appears to be partially responsible for mediating phosphoramidate and lysyl-AMP substrate specificity, providing important information for the possible design of antitumor, antiviral, and antibacterial pronucleotides (3). In addition, the substantial sequence variability of the C termini of Hints is likely to be an important factor governing the species-specific interactions of Hints with aminoacyl-tRNA synthetases and possibly other proteins. The results of ongoing X-ray crystal studies of Hints cocrystallized with substrate-based inhibitors, as well as LysRS, should provide greater insights into the role of the C-terminal loop.

SUPPORTING INFORMATION AVAILABLE

SDS-PAGE and gel filtration chromatogram of purified Hint proteins, the calibration curve for the Superdex 75 10/

300GL column, circular dichroism spectra of the Hint proteins, histogram comparing the second-order rate constants, and a mechanism of phosphoramidate and lysyl-AMP hydrolysis. This material is available free of charge via the Internet at <http://pubs.acs.org>.

REFERENCES

- Bieganowski, P., Garrison, P. N., Hodawadekar, S. C., Faye, G., Barnes, L. D., and Brenner, C. (2002) Adenosine monophosphoramidase activity of Hint and Hnt1 supports function of Kin28, Ccl1, and Tfb3, *J. Bio. Chem.* 277, 10852–10860.
- Chou, T.-F., Bieganowski, P., Shilinski, K., Cheng, J., Brenner, C., and Wagner, C. R. (2005) ³¹P NMR and genetic analysis establish hinT as the only Escherichia coli purine nucleoside phosphoramidase and as essential for growth under high salt conditions, *J. Bio. Chem.* 280, 15356–15361.
- Wagner, C. R., Iyer, V. V., and McIntee, E. J. (2000) Pronucleotides: toward the in vivo delivery of antiviral and anticancer nucleotides, *Med. Res. Rev.* 20, 417–451.
- Chou, T.-F., and Wagner, C. R. (2007) Lysyl-tRNA synthetase-generated lysyl-adenylate is a substrate for histidine triad nucleotide binding proteins, *J. Bio. Chem.* 282, 4719–4727.
- Chou, T.-F., Tikh, I. B., Horta, B. A., Ghosh, B., de Alencastro, R. B., and Wagner, C. R. (2007) Engineered Monomeric Human Histidine Triad Nucleotide Binding Protein 1 Hydrolyzes Fluorogenic Acyl-Adenylate and Lysyl-tRNA Synthetase-generated Lysyl-Adenylate, *J. Bio. Chem.* 282, 15137–15147.
- Brenner, C. (2002) Hint, Fhit, and GalT: function, structure, evolution, and mechanism of three branches of the histidine triad superfamily of nucleotide hydrolases and transferases, *Biochemistry* 41, 9003–9014.
- Butland, G., Peregrin-Alvarez, J. M., Li, J., Yang, W., Yang, X., Canadien, V., Starostine, A., Richards, D., Beattie, B., Krogan, N., Davey, M., Parkinson, J., Greenblatt, J., and Emili, A. (2005) Interaction network containing conserved and essential protein complexes in Escherichia coli, *Nature* 433, 531–537.
- Hopfe, M., Hoffmann, R., and Henrich, B. (2004) P80, the HinT interacting membrane protein, is a secreted antigen of Mycoplasma hominis, *BMC Microbiol.* 4, 46.
- Kitzerow, A., and Henrich, B. (2001) The cytosolic HinT protein of Mycoplasma hominis interacts with two membrane proteins, *Mol. Microbiol.* 41, 279–287.
- Lee, Y. N., and Razin, E. (2005) Nonconventional involvement of LysRS in the molecular mechanism of USF2 transcriptional activity in FcεRI-activated mast cells, *Mol. Cell. Biol.* 25, 8904–8912.
- Lee, Y. N., Nechushtan, H., Figov, N., and Razin, E. (2004) The function of lysyl-tRNA synthetase and Ap4A as signaling regulators of MITF activity in FcεRI-activated mast cells, *Immunity* 20, 145–151.
- Weiske, J., and Huber, O. (2005) The histidine triad protein Hint1 interacts with Pontin and Reptin and inhibits TCF-beta-catenin-mediated transcription, *J. Cell Sci.* 118, 3117–3129.
- Korsisaari, N., and Makela, T. P. (2000) Interactions of Cdk7 and Kin28 with Hint/PKCI-1 and Hnt1 histidine triad proteins, *J. Bio. Chem.* 275, 34837–34840.
- Weiske, J., and Huber, O. (2006) The histidine triad protein Hint1 triggers apoptosis independent of its enzymatic activity, *J. Bio. Chem.* 281, 27356–27366.
- Martin, J., Magnino, F., Schmidt, K., Piguet, A.-C., Lee, J.-S., Semela, D., St-Pierre, M. V., Ziemiecki, A., Cassio, D., Mochly-Rosen, D., Brenner, C., Thorgeirsson, S. S., and Dufour, J.-F. (2006) Hint2, a Mitochondrial apoptotic sensitizer downregulated in hepatocellular carcinoma, *Gastroenterology* 130, 2179–2188.
- Lima, C. D., Klein, M. G., Weinstein, I. B., and Hendrickson, W. A. (1996) Three-dimensional structure of human protein kinase C interacting protein 1, a member of the HIT family of proteins, *Proc. Natl. Acad. Sci. U.S.A.* 93, 5357–5362.
- Lima, C. D., Klein, M. G., and Hendrickson, W. A. (1997) Structure-based analysis of catalysis and substrate definition in the HIT protein family, *Science* 278, 286–290.
- Brenner, C., Garrison, P., Gilmour, J., Peisach, D., Ringe, D., Petsko, G. A., and Lowenstein, J. M. (1997) Crystal structures of HINT demonstrate that histidine triad proteins are GalT-related nucleotide-binding proteins, *Nat. Struct. Biol.* 4, 231–238.
- Chou, T.-F., Baraniak, J., Kaczmarek, R., Zhou, X., Cheng, J., Ghosh, B., and Wagner, C. R. (2007) Phosphoramidate Pronucleotides: A Comparison of the Phosphoramidase Substrate Specificity of Human and E. coli Histidine Triad Nucleotide Binding Proteins (Hint1), *Mol. Pharmaceutics* 4, 208–217.
- Ghosh, S., and Lowenstein, J. M. (1996) A multifunctional vector system for heterologous expression of proteins in Escherichia coli, *Gene* 176, 249–255.
- Chang, S. L., Griesgraber, G. W., Southern, P. J., and Wagner, C. R. (2001) Amino acid phosphoramidate monoesters of 3'-azido-3'-deoxythymidine: relationship between antiviral potency and intracellular metabolism, *J. Med. Chem.* 44, 223–231.
- Pearson, J. D., DeWald, D. B., Mathews, W. R., Mozier, N. M., ZurcherNelly, H. A., Heinrikson, R. L., Morris, M. A., McCubbin, W. D., McDonald, J. R., Fraser, E. D., Vogel, H. J., Kay, C. M., and Walsh, M. P. (1990) Amino acid sequence and characterization of a protein inhibitor of protein kinase C, *J. Bio. Chem.* 265, 4583–4591.
- Li, H., Zhang, Y., Su, T., Santella, R. M., and Weinstein, I. B. (2006) Hint1 is a haplo-insufficient tumor suppressor in mice, *Oncogene* 25, 713–721.
- Yuan, B. Z., Jefferson, A. M., Popescu, N. C., and Reynolds, S. H. (2004) Aberrant gene expression in human non small cell lung carcinoma cells exposed to demethylating agent 5-aza-2'-deoxycytidine, *Neoplasia* 6, 412–429.
- Su, T., Suzui, M., Wang, L., Lin, C. S., Xing, W. Q., and Weinstein, I. B. (2003) Deletion of histidine triad nucleotide-binding protein 1/PKC-interacting protein in mice enhances cell growth and carcinogenesis, *Proc. Natl. Acad. Sci. U.S.A.* 100, 7824–7829.

BI701244H